Jet-Wing Lifting-Surface Theory Using Elementary Vortex Distributions

C. C. Shen*, M. L. Lopez†, and N. F. Wasson‡
Douglas Aircraft Company, McDonnell Douglas Corporation, Long Beach, Calif.

A lifting-surface theory for jet wings based on a finite-element method—the method of elementary vortex distribution or the EVD method—is presented. The method utilizes a set of independent but overlapped elementary horseshoe vortex distributions to represent the wing and jet sheet, and satisfies a set of mixed-type boundary conditions on both the wing and jet sheet. The solution includes chordwise and spanwise loading distributions, from which sectional and total aerodynamic quantities (e.g., lift, pitching moment, induced drag, etc.) are derived. In view of the finite-element approach, the method can, in general, be applied to jet wings of arbitrary planform, camber, twist, partial-span flaps, and arbitrary trailing-edge jet-momentum distribution. The present method also reduces to a conventional lifting-surface theory when the jet momentum is zero. An extensive comparison has been made of solutions derived with the EVD method with other theoretical and experimental data for jet wings and conventional wings. Good agreement has been observed in the chordwise and span-wise loadings as well as total aerodynamic coefficients.

Nomenclature

AR = aspect ratio (b^2/S)
b = wing span length
c = chord length of a wing section
C_{D_i}, c_{d_i} = total and sectional induced drag coefficients
C_J, c_μ = total and sectional jet momentum coefficient
C_L, c_ℓ = total and sectional lift coefficient
$C_{L_\Gamma}, c_{\ell_\Gamma}$ = total and sectional lift coefficient due to circulation (pressure) only
c_s = sectional leading-edge suction coefficient (in x-direction)
J = jet momentum flux
p = pressure
q = magnitude of velocity
R = longitudinal radius of curvature of the jet sheet
S = wing planform reference area
U = freestream velocity
u = x-component of perturbation velocity
w = downwash velocity
x,y,z = Cartesian coordinates defined for the jet-wing problem
$\bar{x}$ = x-distance from the leading edge in terms of a fraction of chord
$\bar{x}_{c.p.}$ = sectional center of pressure location from the leading edge in terms of a fraction of chord
$\bar{z}$ = deflection of the jet path
x_ℓ = x-coordinate of the wing leading-edge point
x_t = x-coordinate of the wing trailing-edge point
α = angle of attack
α_{i_∞} = downwash angle or jet angle at infinity downstream relative to the freestream direction
β = deflection angle of flap or jet
Γ = total circulation around a jet-wing section
γ = horseshoe velocity strength
ΔC_p = loading (or the pressure difference) coefficient
δ_J = jet deflection angle relative to the slope of the wing trailing edge
θ = jet deflection angle with respect to the freestream direction
ϵ = local incidence angle at a point on the wing
$\Lambda_{c/4}$ = wing quarter-chord-line sweepback angle
λ = wing taper ratio
ρ = density of freestream flow
ξ,η,ζ = Cartesian coordinates (dummies for x, y, z)

Presented as Paper 73-652 at the AIAA 6th Fluid and Plasma Dynamics Conference, Palm Springs, Calif., July 16-18, 1973; submitted October 4, 1973; revision received October 21, 1974. This work was performed under the sponsorship of the Independent Research and Development Program of the McDonnell Douglas Corporation and the Office of Naval Research Contract 00014-71-C-0250.

Index category: Aircraft Aerodynamics (including Component Aerodynamics).

*Senior Engineer/Scientist, Viscous Flows Research, Aerodynamics Subdivision. Member AIAA.

†STOL Program Office, Advance Design Division.

‡Engineer/Scientist, Powered Lift Systems Aerodynamic Technology.

Introduction

MANY high-lift systems developed for STOL transport aircraft utilize the jet-flap principle; for example, the internally-ducted jet flap, the externally-blown jet flap, the upper surface blowing jet flap and augmentor wing. To cope with the need for methods for the aerodynamic design and analysis of these systems, the present method—a jet-wing lifting-surface theory—is developed, which is generally applicable to jet wings of arbitrary geometry trailed by a jet sheet of arbitrary momentum distribution. The term "jet-wing" is used here as an abbreviation for "jet-flapped wing."

Past developments of analytical methods for calculating the loading distribution of jet wings of finite aspect ratio include those by Kuchemann,[1] Maskell and Spence,[2] Yoler,[3] Lopez,[4] Das,[5] Erickson and Kaskel,[6] and Tokuda.[7] Each of these methods has some limitations that prevent it from being considered suitable for application to complex jet-wing configurations. The Kuchemann[1] method, for example, presents only an approximate procedure for evaluating the pressure distribution of a jet wing of nonzero thickness. Maskell and Spence[2] have formally formulated a jet-wing lifting-surface theory which assumes elementary horseshoe vortices originating from both the wing and jet sheet, but the method employed by them to solve such a theory is similar to the Prandtl lifting-line method. Moreover, their solution is limited to the very special case where the spanwise loading, chord length, and jet momentum all assume elliptical distributions, and the jet deflection and sectional incidence (twist) are held constant over then span. Yoler[3] provided a modified, lifting-line method which includes two vortex lines fixed at the quarter-chord and three-quarter-chord lines of the wing. The Maskell and Spence method was also extended by Lopez[4] for solutions of arbitrary jet wings of high aspect ratio. A more rigorous treatment of the lifting-surface problem was given by Das.[5] A loading function technique was adopted along with the use of certain jet-flap charac-

teristics derived from Spence's[8] two-dimensional jet-flap solution. The boundary conditions are satisfied at only three points in a chordwise section; namely, the quarter-chord and three-quarter-chord points, and infinity downstream. Because of this limitation, the method is not normally regarded as satisfactory when there is a variation of chordwise geometry of the wing, such as camber and flap deflections. Finally, Erickson and Kaskel[6] treat rectangular jet wings of low aspect ratio, and Tokuda[7] constructed a uniformly valid asymptotic solution for high-aspect-ratio jet wings by using the method of asymptotic expansions.

The present method employs a finite-element scheme, which enables a jet wing of an arbitrary geometry with camber, partial-span flap, partial-span blowing, etc. to be conveniently and properly treated. This method assumes a piecewise continuous horseshoe vortex distribution in the chordwise direction, and appropriate singularity at the leading edge, the flap hinge line, and the jet deflection line of the wing. As a result of such assumption, the induced downwash calculated is either continuous in the chordwise direction or possesses appropriate jump across the hinge line or the deflection line. The continuity condition in vorticity distribution is relaxed in the spanwise direction for simplifying calculations; however, this does not seem to provide a serious drawback in the solution. An important feature of the present method arises from the assumption of the leading edge singularity of vorticity distribution, which enables the leading edge suction and hence the induced drag to be determined accurately.

A brief description and some results of the present method were first given in Ref. 4. A complete description of the theory, its extension to the calculation of dynamic derivatives, and the associated computer program are presented in Ref. 9.

Jet-Wing Lifting-Surface Theory

The basic aerodynamic principle of the jet flap has been well established. The presence of the thin jet sheet behind the wing greatly affects the pressure distribution around it and normally results in an increase in lift that may be several times greater than that possible with the wing alone. The shape of the jet sheet, which determines these changes, is in itself a function not only of magnitude and distribution of jet momentum but also of the configuration of the wing. In view of this strong and inseparable interaction, any analysis of a jet wing inherently requires that the wing and jet be treated as an integrated system, from which the pressure distribution on the wing and the shape of the jet sheet are solved simultaneously.

The distinction between the jet-wing problem and the conventional wing problem naturally lies in the jet sheet. In the case of the jet-wing problem, a dynamic boundary condition must be satisfied on the jet sheet in addition to a kinematic boundary condition required to be satisfied on the wing. These two boundary conditions constitute the so-called mixed type boundary-value problem, which is considerably difficult to solve. Another difficulty arises because of the infinite extent of the jet sheet. The boundary region, instead of being the usual finite size, becomes semi-infinitely large. Despite these difficulties, a theoretical model based on the lifting-surface concept has been sufficiently well established in the past, and limited solutions have been derived by several authors. This theoretical model, as first prescribed by Maskell and Spence,[2] is illustrated in Fig. 1.

Analogous to the classical thin-wing theory, it is assumed that the thickness of the jet sheet, in addition to that of the wing, is zero. The jet-sheet, on the other hand, possesses a finite momentum flux and can sustain a discontinuity of pressure. In other words, the calculation is based on the mean camber surface of the wing and the mean location of the jet sheet. A restriction is also imposed that no transverse transport of momentum takes place within the jet sheet, so that the jet flow can be considered to lie in streamwise planes. The momentum flux is considered constant along the jet in each streamwise plane.

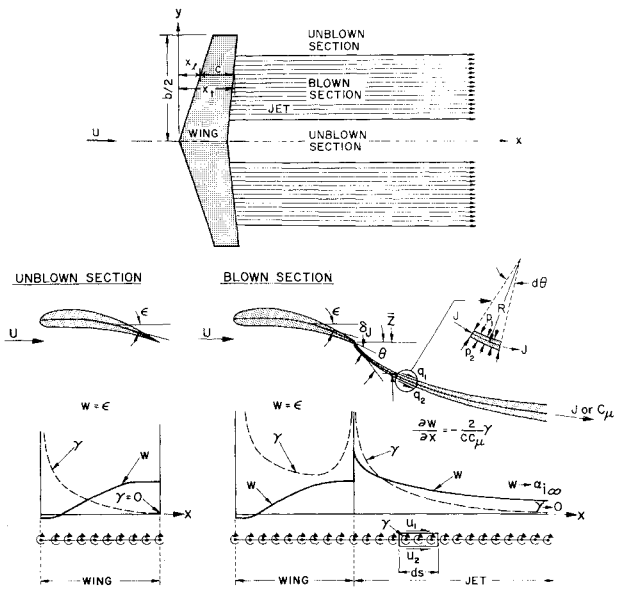

Fig. 1 Theoretical model of jet wing.

Assume an incompressible, inviscid flow of freestream velocity U past the jet-wing system as shown in Fig. 1. First consider the dynamic boundary condition on the jet, which gives the pressure jump p_2-p_1 across the jet in terms of the jet momentum flux $J(y)$ and the radius of curvature R of the jet path; that is,

$$p_2-p_1=J/R \tag{1}$$

This relation may be viewed as a balance of the pressure and centrifugal forces acting on an element of the jet. On using the Bernoulli equation, Eq. (1) may also be written in terms of the velocity jump as follows:

$$q_1^2-q_2^2=2J/\rho R \tag{2}$$

where q_1 and q_2 signify the magnitudes of the total velocity on the upper and lower surfaces of the jet, respectively, and ρ denotes the density of the external flow.

The dynamic boundary condition above is nonlinear in nature. To render the solution more tractable the present jet-wing problem is linearized. As in classical lifting surface theory, all angular deflections are taken to be small. The boundary conditions are satisfied at the displaced locations; in this case, the projection of the jet wing onto the $z=0$ plane passing through the apex of the wing.

In accordance with this linear approximation, the kinematic boundary condition on the wing is a familiar one; that is,

$$w/U=\epsilon \tag{3}$$

where w designates the downwash velocity and ϵ the local incidence or slope of the wing. Likewise, the kinematic boundary condition on the jet may be written as

$$w/U=-\partial\bar{z}/\partial x \tag{4}$$

where $\bar{z}(x,y)$ represents the deflection of the jet path.

When the jet path is shallow, the curvature $1/R$ may be approximated by $\partial^2\bar{z}/\partial x^2$, which, on account of Eq. (4), can be written as

$$1/R\simeq\partial^2\bar{z}/\partial x^2=-(1/U)\partial w/\partial x \tag{5}$$

With this approximation and $q_1^2-q_2^2\simeq 2U(u_1-u_2)$, the dynamic boundary condition, Eq. (2), is conveniently reduced to the following linearized form:

$$u_1-u_2=-(cc_\mu/2)\partial w/\partial x \tag{6}$$

in which c_μ is the sectional jet momentum coefficient defined as follows:

$$c_\mu = J(y)/\tfrac{1}{2}\rho U^2 c \tag{7}$$

where c denotes the local chord length. A total jet momentum coefficient C_J is also defined as follows:

$$C_J = \frac{1}{S}\int_{-b/2}^{b/2} c c_\mu \mathrm{d}y \tag{8}$$

where b represents the wing span length and S the wing reference area.

In a lifting problem, the Kutta condition must also be imposed. On unblown sections of the wing, naturally, the Kutta condition must be satisfied at the trailing edge of the wing. On blown sections where the jet sheet acts like an extension of the wing, the Kutta condition must be satisfied at infinity downstream on the jet sheet. Since the Kutta condition requires the velocity to be finite, it may be expressed as

$$u_1 - u_2 = 0 \tag{9}$$

in the present linearized sense.

Furthermore, the jet path can have a specified angular deflection at the wing trailing edge. If this jet angle with respect to the freestream direction is θ, the streamline condition on this initial point of the jet, again in the linearized sense, requires that

$$w/U = \theta \tag{10}$$

The linear jet-wing problem as described above may be solved by using a distribution of singularities. As in classical lifiting-surface theory, infinitesimal horseshoe vortices are adopted. They are assumed to originate from the wing and also from the jet sheet. The horseshoe vorticity strength γ is, of course, related to the velocity jump across the vortex sheet as follows:

$$u_1 - u_2 = \gamma \tag{11}$$

Based on the horseshoe-vortex representation, all the equations pertinent to the jet-wing problem may be written in terms of γ. These equations are summarized below in their normalized forms (γ and w are normalized with respect to U, all lengths with respect to the wing semi-span $b/2$. All the normalized variables will retain their original symbols):

$$w(x,y) = \epsilon(x,y) \quad (z=0, \text{ wing boundary}) \tag{12}$$

$$\frac{\partial w(x,y)}{\partial x} = -\frac{2}{c(y)c_\mu(y)}\gamma(x,y) \quad (z=0, \text{ jet boundary}) \tag{13}$$

$$w(x,y) = \theta(y) \quad [x = x_t^+(y), \text{ where } c_\mu(y) \neq 0] \tag{14}$$

$$\gamma(x,y) = 0 \qquad (x \to \infty, \text{ where } c_\mu(y) \neq 0)$$
$$(x = x_t^-(y), \text{ where } c_\mu(y) = 0) \tag{15}$$

In the above the — and + signs on x_t indicate the points on the wing and jet sides, respectively, of the wing trailing edge. The downwash w is considered to be induced by the horseshoe vortices only, with the downwash-vorticity relation being given by the following well-known equation:

$$w(x,y) = -\frac{1}{4\pi}\oint_{-1}^{+1}\frac{d\eta}{(y-\eta)^2} \times \int_{x_{hp\ell}}^{x_t \text{ or } \infty}\gamma(\xi,\eta)\left(1+\frac{x-\xi}{r}\right)d\xi \tag{16}$$

where

$$r = [(x-\xi)^2 + (y-\eta)^2 + (z-\zeta)^2]^{1/2}$$

The upper limit of the ξ-integral is either $x_t(\eta)$ or ∞, depending on whether or not $c_\mu(\eta) = 0$. The cross sign on the η-integral indicates that the principle value is to be taken.

Equations (12-16) constitute the formulation of the jet-wing lifting-surface theory. They are to be solved simultaneously for the vorticity strength $\gamma(x,y)$, following which all aerodynamic characteristics are derived in terms of γ.

Methods of Elementary Vortex Distribution

Finite-Element Concepts

In view of the complexity that the geometry of a modern wing may involve, and in order to allow flexibility in distributing the jet, the solution of the jet-wing theory necessarily resorts to a finite-element approach. In general, a finite-element method approximates the jet-wing boundary by a large but finite number of small elements. Over these elements, a set of independent vortex distributions or discrete vortices of unknown magnitudes is presented. The result of the combined distributions is to give the theoretical distribution of vorticity over the jet-wing boundary. The boundary conditions, instead of being satisfied continuously over the boundary, are required to be satisfied at only one point of each element.

In dealing with conventional wings, several finite-element schemes have been developed with varying degrees of success. In the vortex lattice method, for example, a discrete horseshoe vortex, with its bound vortex located at the quarter-interval line, represents the vortex distribution in each element which can be quadrilateral in shape. An alternative approach is the "box" method in which a constant vortex distribution is assumed over the element. Both of these schemes possess, however, the inherent drawback that the vortex induced downwash is artificially singular in many places. For example, the downwash becomes infinitely large when approaching a discrete vortex or, in the case of a constant vortex distribution, at the junction of two neighboring elements where a discontinuity of vorticity prevails. This behavior is best illustrated in the two dimensional case shown in Fig. 2. The two vortex representations and their associated downwash distributions are presented for a flat plate at an angle of attack. The resulting downwash curves are seen to depart radically from the theoretical value of unity except at one or two places in each element. This explains the reason why the solution by either of the above two methods requires the careful selection of the location of the control point in each element where the boundary condition is to be satisfied. A more in-depth evaluation of finite-element schemes is discussed in Ref. 10.

On the other-hand, if the vorticity of the flat plate is represented by a piecewise linear and continuous distribution, incorporating an appropriate asymptotic behavior at the leading edge, the resulting downwash is bounded everywhere and very close to unity. This scheme and its associated downwash distribution is also illustrated in Fig. 2 under the label of the EVD model. Notice that the original piecewise distribution can be replaced by a set of overlapped elementary vortex distributions (EVD's). The finite-element scheme using the EVD's will be termed the method of elementary vortex distribution, hereafter abbreviated as the EVD method. The EVD method does not require the control point to be selected in any particular way. Because of this important feature, this method has been adopted for the three-dimensional jet-wing analysis.

Elementary Vortex Distributions

In the three-dimensional case, the jet-wing boundary (on the $z=0$ plane) is divided into chordwise strips parallel to the

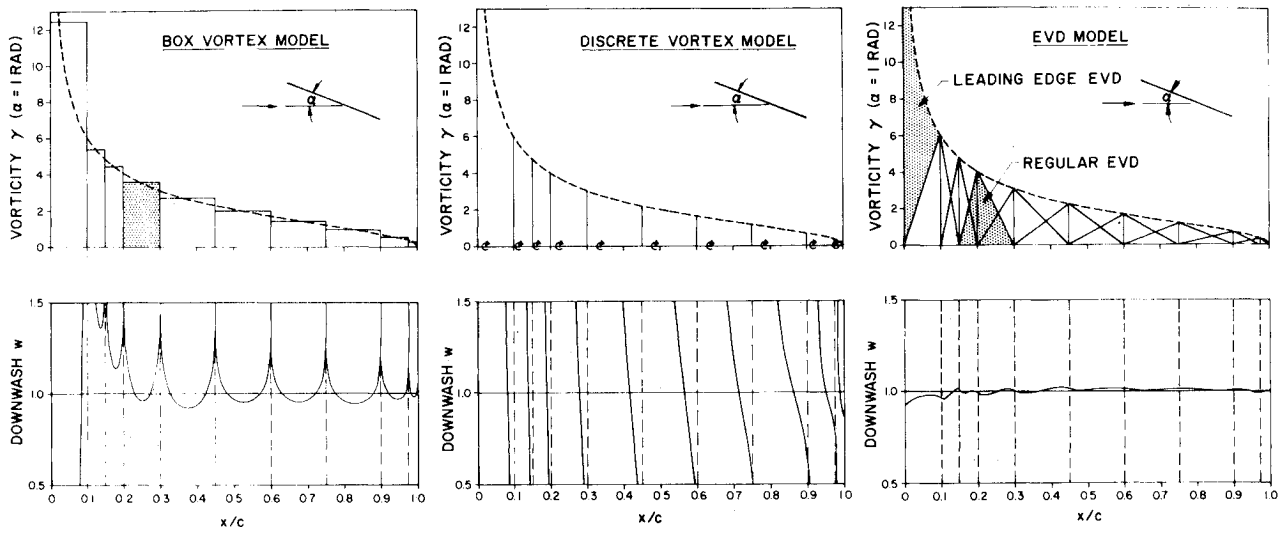

Fig. 2 Three vortex models applied to a flat-plate airfoil.

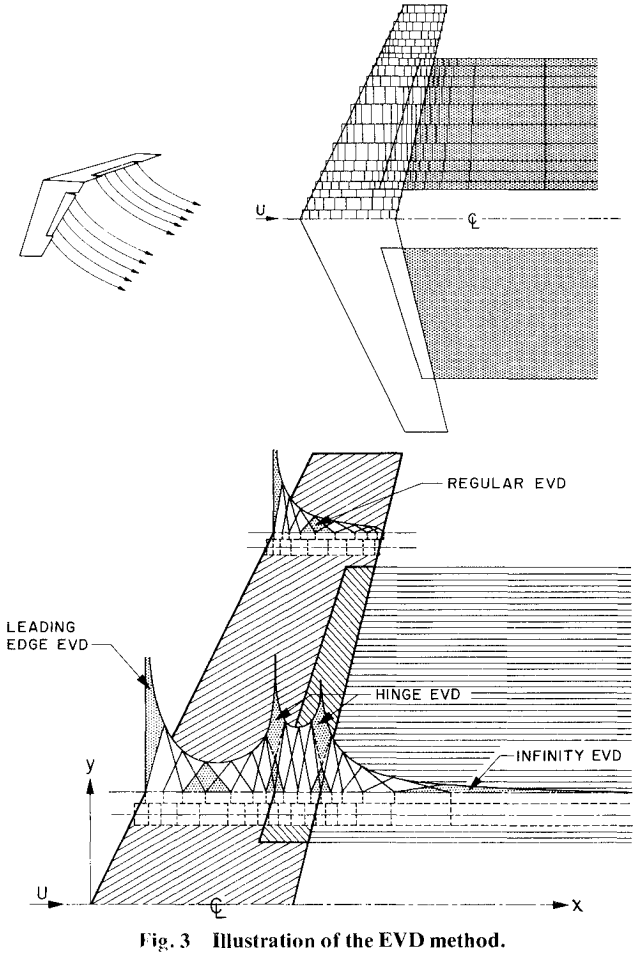

Fig. 3 Illustration of the EVD method.

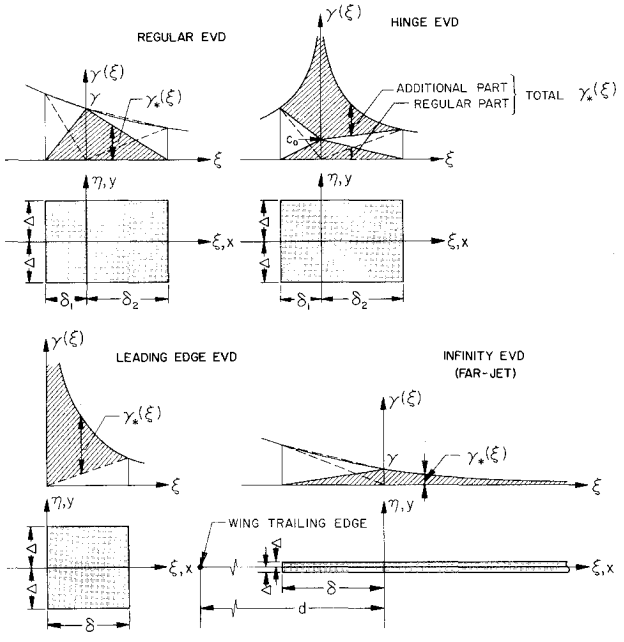

Fig. 4 Elementary vortex distributions.

freestream, and subsequently each strip is subdivided into a number of small rectangular elements. Figure 3 demonstrates the procedure. The use of rectangular elements is for simplifying the calculations. Although such an arrangement might be criticized in that it cannot truly represent the planform of a swept wing, the results of caluclations here shown that the use of rectangular elements does not present a serious restriction as long as a sufficient number of elements is used.

The jet-wing vortex distribution can now be represented by a series of elementary vortex distributions (EVD's), each distributed over one or two elements. The EVD's are overlapped chordwise, as illustrated in Fig. 3, to produce a piecewise linear and continuous vortex distribution (including proper singular behavior wherever necessary) in a chordwise direction. For the sake of simplifying calculation, however, the spanwise vortex distribution is assumed piecewise constant and hence is discontinuous. Four types of EVDs are used; they are defined as follows (shown in Fig. 4):

1) Regular EVD

The regular EVD is associated with the majority of the elements. It is triangular in shape and distributed over two successive elements. In terms of local coordinates, the regular EVD is expressed as

$$\gamma_*(\xi,\eta)=\begin{cases}\gamma(\xi+\delta_1)/\delta_1, & (-\delta_1\le\xi\le 0, |\eta|\le\Delta)\\ -\gamma(\xi-\delta_2)/\delta_2, & (0\le\xi\le\delta_2, |\eta|\le\Delta)\end{cases} \tag{17}$$

where γ represents the local vortex strength at the junction of the two elements.

2) Leading-Edge EVD

Consistent with classical lifting-surface theory, a leading-edge EVD of square-root singular behavior is adopted for the

leading-edge elements. It is expressed by

$$\gamma_*(\xi,\eta)=\bar{\gamma}(2/3)[(\xi/\delta)^{-1/2}-(\xi/\delta)],(0<\xi\leq\delta,|\eta|\leq\Delta) \quad (18)$$

where $\bar{\gamma}$ indicates the mean value of this EVD.

3) Hinge EVD

As is well known from linearized thin-airfoil and jet-flap theory, the vortex distribution over a flap hinge or jet deflection line is logarithmically singular and its strength is proportional directly to the angle of deflection. Therefore, over any two elements adjacent to a deflection line, a hinge EVD will be adopted. It consists of two parts: a regular EVD of unknown magnitude and an additional hinge EVD of singular nature but of known strength; that is,

$$\gamma_*(\xi,\eta)=\gamma_1(\xi,\eta)+\gamma_2(\xi,\eta)$$

The regular part γ_1 has the same form as Eq. (17), while the additional part γ_2 can be expressed as follows:

$$\gamma_2(\xi,\eta)=\begin{cases}-2\beta/\pi(\log|\xi|+\xi\log\delta_1/\delta_1), \\ \quad(-\delta_1\leq\xi<0,\ |\eta|\leq\Delta) \\ -2\beta/\pi(\log|\xi|-\xi\log\delta_2/\delta_2), \\ \quad(0<\xi\leq\delta_2,\ |\eta|\leq\Delta)\end{cases} \quad (19)$$

where β is the deflection angle of the flap or jet.

4) Infinity EVD

An important feature of the EVD method is that it is not necessary to truncate the jet. This is achieved through the use of a semi-infinitely long element at the downstream end of the jet. The infinity EVD, which represents the appropriate decay in vorticity, is associated with this element. It includes a linear distribution from the preceding element and is expressed as

$$\gamma_*(\xi,\eta)=\begin{cases}\gamma(\xi+\delta)/\delta,(-\delta\leq\xi\leq0,\ |\eta|\leq\Delta) \\ \gamma(\xi/d+1)^{-2},(\xi\geq0,\ |\eta|\leq\Delta)\end{cases} \quad (20)$$

where γ is again the local vortex strength at the junction of the two elements, and d represents the distance from the wing trailing edge to the junction. Incidently, this EVD contains a finite amount of total vorticity and satisfies the Kutta condition at infinity.

Downwash Influence Coefficients

It will be noted that each EVD contains only one unknown coefficient. In general, the expression for the jth EVD can be written as

$$\gamma_{*j}(\xi,\eta)=\gamma_j g_j(\xi)+\beta_j h_j(\xi) \quad (21)$$

where the second term is a known quantity representing the additional Hinge EVD. This term vanishes when no deflection of any kind is involved (i.e., $\beta_j=0$).

The downwash at any point due to an EVD can be calculated according to the downwash-vorticity relationship similar to that given by Eqs. (16), or explicitly,

$$w_{ij}=a_{ij}\gamma_j+b_{ij}\beta_j \quad (22)$$

where

$$a_{ij}=-\frac{1}{4\pi}\iint_{\Delta A_j}\frac{g_j(\xi)}{(y_i-\eta)^2}\left(1+\frac{x_i-\xi}{r_i}\right)d\xi d\eta \quad (23)$$

$$b_{ij}=-\frac{1}{4\pi}\iint_{\Delta A_j}\frac{h_j(\xi)}{(y_i-\eta)^2}\left(1+\frac{x_i-\xi}{r_i}\right)d\xi d\eta \quad (24)$$

The coefficients a_{ij} and b_{ij} are known as downwash influence coefficients; that is, the downwash at the i-th point due to the jth EVD of unit magnitude (expressed by the functions g_j and h_j). The integrations are performed over the element or elements over which the jth EVD is defined.

The downwash influence coefficients for each type of EVD have been integrated analytically. The resulting expressions are too lengthy to include here. They are, however, presented in Refs. 9 and 10. In the case of the leading-edge and additional hinge EVD, the integrands are organized into a singular and a continuous part, the latter being integrated by the Gaussian quadrature. The downwash distribution due to each individual EVD is itself continuous everywhere apart from the element edges parallel to the chord.

The total downwash at the ith point is obtained from a summation of the incremental downwash due to all EVD's; that is,

$$w_i=\sum_{j=1}^{N}a_{ij}\gamma_j+\sum_{j=1}^{N}b_{ij}\beta_j \quad (25)$$

where N is the total number of EVD's.

Boundary Conditions

The boundary conditions are now applied to the control points, one for each element. In the EVD scheme, the control point is chosen to locate in the mid-span of the element to avoid encountering edge singularities; otherwise, it is totally arbitrary with respect to the chordwise location.

The boundary conditions were given before as Eqs. (12-15). On substitution of the downwash expression, Eq. (25), the wing boundary condition, Eq. (12), applied at the $i$the control point can be written as

$$\sum_{j=1}^{N}a_{ij}\gamma_j=\epsilon_i-\sum_{j=1}^{N}b_{ij}\beta_j(i,\text{ on wing}) \quad (26)$$

To convert the jet boundary condition into a numerical form, Eq. (13) is integrated over a small distance along the jet, from the $(i-1)$th to ith control point, to give

$$w_i-w_{i-1}=-\frac{2}{c(y_i)c_\mu(y_i)}\int_{x_{i-1}}^{x_i}\gamma(\xi)d\xi\ (i,\text{ on jet}) \quad (27)$$

If the integral on the right-hand side of the equation is replaced by

$$\int_{x_{i-1}}^{x_i}\gamma(\xi)d\xi=\sum_{j=1}^{N}e_{ij}\gamma_j+\sum_{j=1}^{N}f_{ij}\beta_j, \quad (28)$$

the boundary condition at the i-th control point on the jet becomes

$$\sum_{j=1}^{N}[a_{ij}-a_{i-1,j}+v(y_i)e_{ij}]\gamma_j= -\sum_{j=1}^{N}[b_{ij}-b_{i-1,j}+v(y_i)f_{ij}]\beta_j(i,\text{ on jet}) \quad (29)$$

where $v(y_i)$ is a jet momentum quantity defined by

$$v(y_i)=2/c(y_1)c_\mu(y_i) \quad (30)$$

The values of the integration coefficients e_{ij} and f_{ij} depend on the choice of the control point location relative to an element; however, they can be easily derived once the control point is defined. References 9 and 10 include a set of expressions for these coefficients corresponding to the control point given at the center of the element.

A special situation arises when the control point is the leading one on the jet just behind the trailing edge of the wing. In this case the integration of Eq. (13) has to start from the trailing edge ($x=x_t$), because this equation does not apply to the wing. Replacing x_{i-1} by $x_t(y_i)$ and w_{i-1} by the initial jet angle $\theta(y_i)$ in Eq. (27) results in

$$\sum_{j=1}^{N} [a_{ij}+v(y_i)e_{ij}]\gamma_j=\theta(y_i)-\sum_{j=1}^{N} [b_{ij}+v(y_i)f_{ij}]\beta_j$$

(i, leading control point on jet) (31)

Because of the substitution of $\theta(y_i)$ into Eq. (31), the boundary condition for the initial portion of the jet, given by Eq. (14), has been effectively satisfied. The Kutta condition, Eq. (15), need not be considered separately either, since it has already been incorporated into the appropriate EVD. For example, at the wing trailing edge of an unblown section, the use of a regular EVD guarantees that γ is zero there; while at infinity on the jet, γ, as prescribed by the infinity EVD, also vanishes.

Equations (26), (29), and (31) constitute the complete set of equations necessary for solving the jet-wing problem. As there are as many EVD's as there are elements, there are N equations to be solved for N unknowns. The unknown γ_j's largely represent the local vortex strength, while some are the mean values.

Linear Equations

Since the equations of solution are linear in γ_j's, they are summarized below in a matrix form:

$$\sum_{j=1}^{N} A_{ij}\gamma_j=B_i \quad (i=1,2,\ldots N) \tag{32}$$

where the coefficient matrix A_{ij} is

$$A_{ij}=\begin{cases} a_{ij} & (i, \text{ on wing}) \\ a_{ij}+v(y_i)e_{ij} & (i, \text{ leading control point on jet}) \\ a_{ij}-a_{i-1,j}+v(y_i)e_{ij} & (i, \text{ other control points on jet}) \end{cases}$$

and the column matrix B_i is

$$B_i=\begin{cases} \epsilon_i-\sum_{j=1}^{N} b_{ij}\beta_j & (i, \text{ on wing}) \\ \theta(y_i)-\sum_{j=1}^{N} [b_{ij}+v(y_i)f_{ij}]\beta_j & \\ \quad (i, \text{ leading control point on jet}) & \\ \quad -\sum_{j=1}^{N} [b_{ij}-b_{i-1,j}+v(y_i)f_{ij}]\beta_j & \\ \quad (i, \text{ other control point on jet}) & \end{cases}$$

The solution of these equations may be readily achieved by using a digital computer.

Aerodynamic Characteristics

The EVD method, as outlined in the previous section, solves for the vortex strength at a large number of discrete points distributed over the wing and jet sheet. The singular behavior of the vortex distribution near the leading-edge and hinge lines is also determined through the use of the leading-edge and hinge EVD's. In effect, the vortex distribution over the entire jet-wing boundary is determined.

The loading, or the pressure difference across the wing and jet sheet, can be shown to be directly proportional to the vorticity strength by an applications of the Bernoulli equation and vorticity definition. In coefficient form, the loading is

$$\Delta C_p=2\gamma \tag{33}$$

Therefore, the loading distribution is also known over the entire wing and jet sheet.

With the loading distribution known, any force and moment quantity associated with the wing can be readily derived by a straightforward integration of the loading distribution over the wing. These include the sectional as well as the total values of lift, pitching moment, induced drag, and side force, and also the total rolling and yawing moments of the wing. In the case of a jet wing, in addition to the contribution from the pressure loading, which is sometimes termed the circulation contribution, the aerodynamic forces and moments also include a contribution from the jet reaction. For example, the sectional lift coefficient c_ℓ may be expressed as

$$c_\ell=c_{\ell_\Gamma}+c_{\ell_\mu} \tag{34}$$

which is a summation of a circulation term c_{ℓ_Γ} and a jet reaction term c_{ℓ_μ}. Compatible with the linear approach, these terms are, respectively, given by

$$c_{\ell_\Gamma}(y)=\int_0^1 \Delta C_p(\bar{x},y)d\bar{x} \tag{35}$$

and

$$c_{\ell_\mu}(y)=c_\mu(y)\theta(y) \tag{36}$$

where $\bar{x}=(x-x_\ell)/c$ is measured in terms of a fraction of the local chord.

Since the present formulation is based on thin-wing theory, there also exists a leading-edge suction force. Although a second-order quantity compared with the lift, it must be taken into account in the calculation of induced drag, side force, and yawing moment. One of the advantages associated with the EVD method is its ability to determine the leading-edge suction directly from the EVD solution. As the leading-edge suction is solely dependent on the square-root singular behavior of the leading-edge vortex distribution, its value may be determined in terms of the leading-edge EVD strength. Based on a two-dimensional analogy, the following expression for the sectional leading-edge suction c_s has been obtained:

$$c_s=\frac{2}{9}\pi\frac{\delta_\ell}{c}\bar{\gamma}_\ell^2 \tag{37}$$

where δ_ℓ denotes the leading-edge element length, c the chord, and $\bar{\gamma}_\ell$ the mean vortex strength of the leading-edge EVD.

The induced drag is herewith defined as the deficiency in the thrust recovery, or the difference between the ideal thrust ($=c_\mu$) and actual theoretical thrust. A sectional induced drag coefficient c_{d_i} includes three terms: a loading term c_{d_Γ}, a leading-edge suction term c_s, and a jet reaction term c_{d_μ}. In other words,

$$c_{d_i}=c_{d_\Gamma}-c_s+c_{d_\mu} \tag{38}$$

where

$$c_{d_\Gamma}(y)=\int_0^1 \Delta C_p(\bar{x},y)\epsilon(\bar{x})d\bar{x} \tag{39}$$

$$c_{d_\mu}(y)=c_\mu(y)\frac{\theta^2(y)}{2} \tag{40}$$

and c_s has already been given by Eq. (37).

The total induced drag C_{D_i}, but not the spanwise distribution (sectional induced drag c_{d_i}), can also be derived by a far-field application of the momentum theorem. This

simply requires that the flow in the Trefftz plane be considered. From the results of such an analysis, it can be shown that

$$C_{D_i} = \frac{1}{2S} \int_{-1}^{+1} c(y) c_{\ell}(y) \alpha_{i\infty}(y) dy \tag{41}$$

where S denotes the wing reference area. The induced downwash angle $\alpha_{i\infty}(y)$ at the discontinuity slit of the jet and trailing vortex sheet in the Trefftz plane is given by

$$\alpha_{i\infty}(y) = \frac{1}{2\pi} \int_{-1}^{+1} \frac{(d\Gamma/d\eta)d\eta}{y-\eta} \tag{42}$$

where Γ is defined as the circulation or the total vorticity in a section of the jet wing; that is,

$$\Gamma(y) = \int_{x_{\ell}(y)}^{\infty} \gamma(x,y) dx \tag{43}$$

Details associated with the numerical evaluation of $\alpha_{i\infty}(y)$ are given in Refs. 9 and 10. This alternate approach provides a cross check of the accuracy of the EVD method in its evaluation of induced drag.

Computer Program

The EVD method has been programed for use on the IBM 360 and CDC 6600 Computers. The Mark II EVD Jet-Wing Computer Program presented in Ref. 9, for example, includes several geometrical input packages, downwash influence coefficient calculation routines, solution of a large system of linear equations, and calculation of various aerodynamic forces and moments. The linear system is solved essentially by the method of successive elimination, but with the aid of external memory devices to reduce the computer core storage required. No instability in the solution has been observed provided that the jet momentum coefficient c_{μ} is greater than 0.01.

The Mark II EVD program has a built-in capability to solve ten geometrical cases simultaneously. This is accomplished by allowing ten columns for the column matrix. The geometrical cases are for a different local incidence distribution only, not for a different planform or a different jet momentum distribution. As the problem is linear, the solution of a particular geometrical or composite case can be considered as a linear combination of the solutions of what are termed fundamental cases. Examples of fundamental cases are angle of attack, wing camber, twist, deflection of one flap, and deflection of jet. The program is made particularly efficient by utilizing this feature.

Results

In order to assess the validity and accuracy of the EVD method, EVD results for various conventional wings and jet wings have been compared with other theoretical solutions as well as experimental data. Some of these comparisons are now discussed.

Elliptical Jet Wings

The special case of a jet wing, with an elliptical planform and elliptical jet momentum distribution (i.e., $c_{\mu}(y)$ = constant), has been solved by Maskell and Spence[2] using a method based on the lifting-line principle. The EVD results of the lift for the same configuration are compared with those of Maskell and Spence in Fig. 5. These include two jet-wing fundamental cases—the angle-of-attack case where the jet emerges tangentially from the wing trailing edge, and the jet deflection case where the jet makes an angle of deflection δ_J with respect to the wing trailing edge while the angle of attack is held at zero.

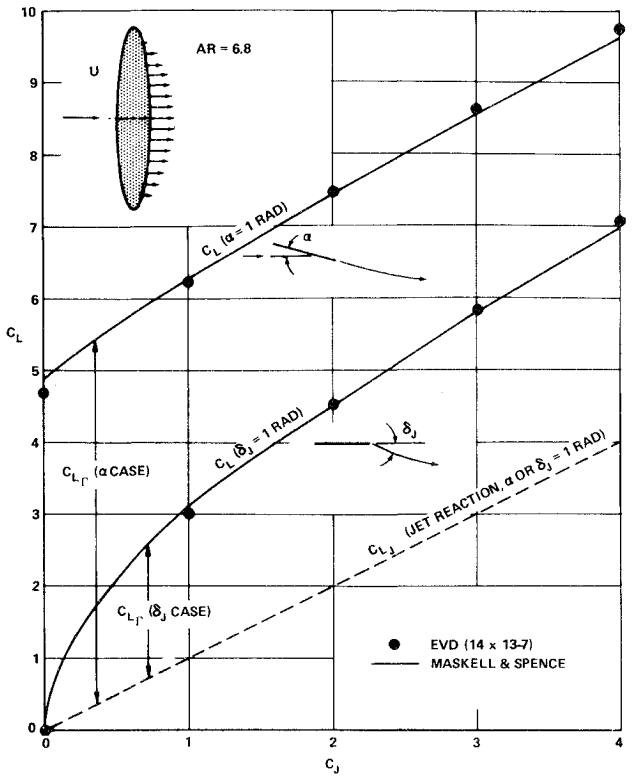

Fig. 5 Comparison of lift for an elliptical jet wing.

The EVD lift characteristics show good agreement with Maskell and Spence's results throughout the range of the jet momentum coefficient C_J studied. Slightly lower lift is obtained with the EVD method when $C_J = 0$ (i.e., a conventional wing) in the angle-of-attack case. This is consistent with the proven fact that the lifting-line theory overpredicts the lift. It should be noted here, that in the EVD calculations, 14 spanwise divisions and 13 chordwise divisions on the wing and 7 on the jet were used. Such a spacing arrangement is indicated in Fig. 5 by "(14×13−7)." This practice of indicating the spacing arrangements will be followed in other figures.

It is also observed from this presentation that the circulation lift C_{L_Γ} almost ceases to increase with increasing jet momentum C_J for C_J's greater than 1; in other words, the jet flap becomes less efficient as a circulation generating device as C_J is increased.

Rectangular Jet Wings

Several jet wings of rectangular planform have been studied extensively by Das[5,11,12] both theoretically and experimentally. Das' wind tunnel tests were performed with a half-span model incorporating an end plate which can be shifted along the span to give effective aspect ratios of 2.75 , 3.5, and 4.5, corresponding to the geometrical aspect ratio of 3,4, and 5, respectively. The model had a chord length of 0.2m and utilized a NACA 0012 airfoil section. It was tested in an open jet wind tunnel with a cross-sectional diameter of 1.3m. A slot of constant width and inclination was installed along the trailing edge of the model to provide jet blowing. Force data were acquired by pressure measurements at several sections of the model.

Comparison of the EVD solutions with Das' theoretical and experimental data are shown in Fig. 6. In general, reasonably good agreement has been observed in the total lift as well as in the spanwise and chordwise loading distributions. Small discrepancies between the two theories may be attributed to the inaccuracy of Das' theory in which several approximations have been introduced. In comparison with the test data, the EVD method underestimates the lift slightly in the angle-of-attack case when C_J is not equal to zero. The dif-

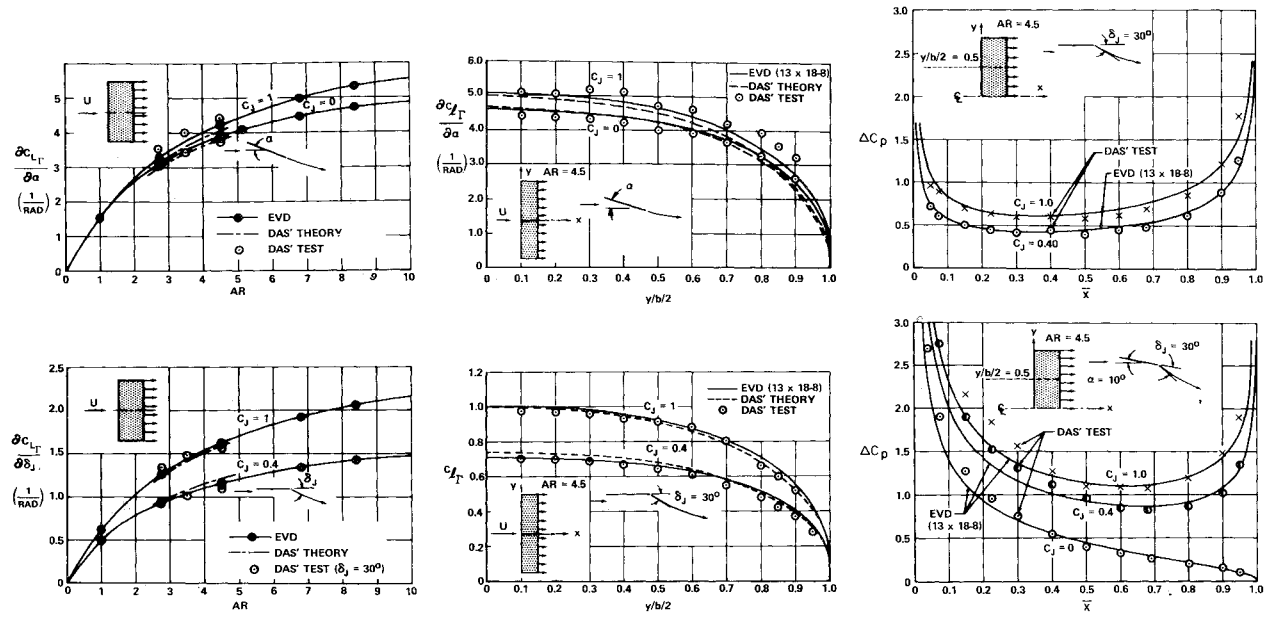

Fig. 6 Comparisons of aerodynamic characteristics for rectangular jet wings.

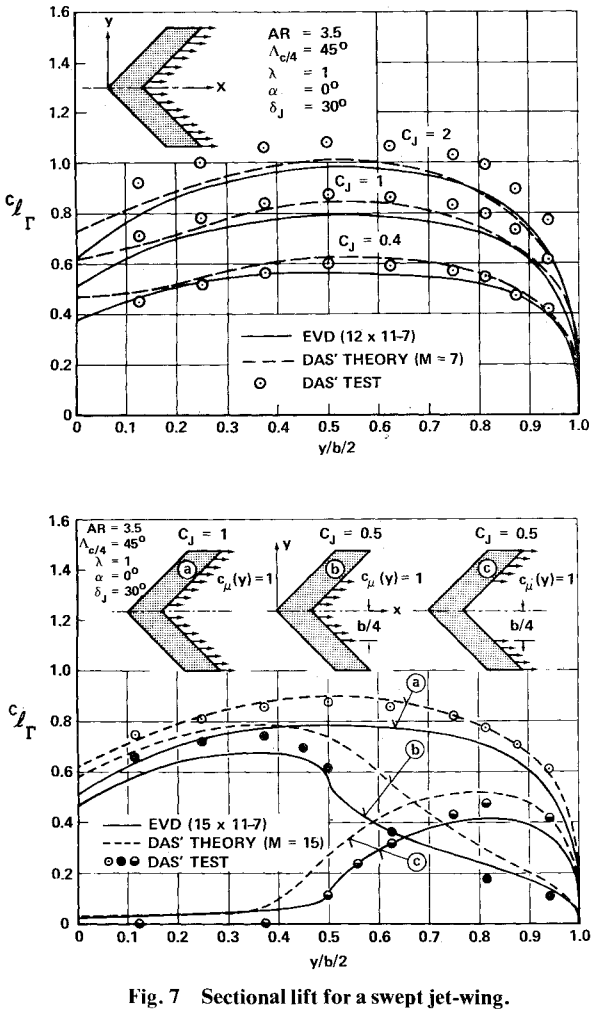

Fig. 7 Sectional lift for a swept jet-wing.

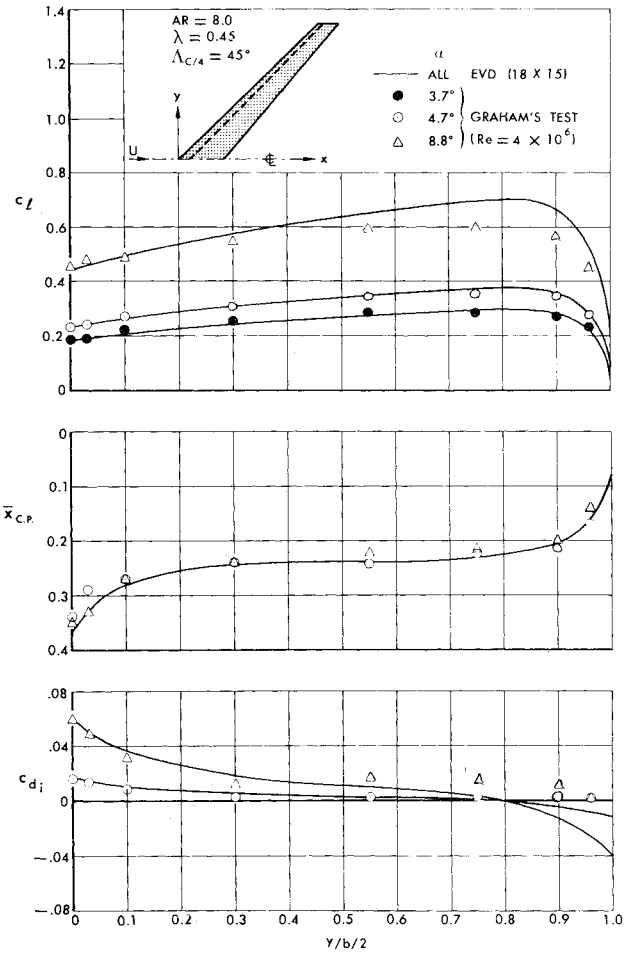

Fig. 8 Sectional aerodynamic characteristics for a tapered swept wing.

ference is associated with a thickness effect which cannot be evaluated directly with the present theory. On the other hand, the seemingly good agreement in the jet deflection case may well be coincidental. The lift increase due to the thickness effect in this case may have been compensated by the loss of lift in the test because the jet deflection angle actually fell below the 30° nominal angle over a portion of span. In fact, discrepancies between the theory and experiment can also be attributed to the effect of the limited size of the wind tunnel, the questionable correction for the end-plate effect, etc.

The EVD method overestimates the lift in the case of no jet blowing ($C_J=0$). The lower experimental values are probably caused by flow separation near the blunt trailing edge of the model, which will not occur in the presence of the

jet. The loss of lift due to separation, in this case, must have exceeded the gain due to the thickness effect.

Swept Jet Wing

Das'[12] has also analyzed and tested a swept jet wing with both full-span and partial-span blowing. Again, a half-span model equipped with an end plate was tested in an open jet wind tunnel. The model has a constant chord of 0.2m, a half span of 0.4m, a sweepback angle of 45°, and a NACA 0012 airfoil section. Following an end-plate correction, the model is considered by Das to have an effective aspect ratio of only 3.5.

Figure 7 shows a comparison of the EVD results for the spanwise circulation lift distribution with those derived from Das' theory and experiment, including full-span, inner-span, and outer-span blowing cases. In all cases, the EVD method tends to underestimate the spanwise circulation lift slightly relative to the test data. The agreement would be much closer, had the EVD solutions been corrected for the effect of thickness as suggested by Spence.[8] For conventional wings, the lift increase due to the thickness effect is about cancelled by the lift loss due to the boundary-layer growth. The jet sucks away the boundary layer, thus creating the need of thickness correction for the jet wings. Das' theory, on the other hand, has overestimated the lift in certain cases and thus, would appear to violate the thickness correction principle. It should be noted that two different spacings were used in Das' calculations, 7 sections for the results presented in the upper drawing of Fig. 7 and 15 sections for the lower one. The two spacings apparently generated quite different results for the same case of full-span blowing with C_J equal to 1.

Tapered Swept Wing

Experiments performed so far on jet wings have all produced results of questionable validity. Thus, the degree of accuracy of the EVD method has been difficult to establish. Complete and accurate measurements, however, exist for conventional wings, for example, the test of a tapered, sweptback wing by Graham.[13] Although the calculation of the aerodynamic characteristics of a conventional wing is not the principal aim of the EVD method, comparison of theory and experiment in this case is still valuable in assuring the general validity of the method.

The wing used in Graham's test had an aspect ratio of 8, taper ratio of 0.45, and quarter-chord sweepback angle of 45°. The calculated and measured results of the sectional lift, center of pressure, and induced drag are compared in Fig. 8. Very good agreement is achieved at the lower angles of attack.

The agreement in the swept-wing results implies that the theoretical solution is consistent with experimental data in spite of the fact that the swept edges of the wing have been approximated by a series of stepped straight edges resulting from the use of rectangular elements.

Conclusions

A lifting surface theory—the EVD method—for the calculation of the aerodynamic characteristics of jet wings has been presented. The versatility of the EVD method is such that wings and jet wings of arbitrary planform geometry, twist, and camber including flaps can be treated. The jet sheet can have an arbitrary spanwise distribution of momentum flux and initial deflection angle. Satisfactory solutions have been obtained with only a moderate number of elements. Hence the computer time involved is also small.

The EVD method is not limited in its application to basic internally ducted jet-flapped wings. It has also been utilized with some success in the evaluation of the aerodynamic characteristics of STOL aircraft configurations which employ, for example, the externally blown jet flap and augmentor or ejector jet-flap wing.[4]

Several extensions to the EVD method have been made since its conception. The aerodynamic characteristics both in and out of ground effect can now be determined, and the stability derivatives due to rolling, pitching, and yawing can be evaluated.[9] It should be noted that in the stability derivative analysis a quasi-steady approach has been used. The vortex distribution obtained from the solution of the EVD method has also been used to calculate the location of the jet sheet as well as the jet-wing flowfield. The extension of the EVD method to enable the analysis of the loading of a jet-wing-fuselage combination, the effect of compressibility, etc., has also been considered.

References

[1]Kuchemann, D., "A Method for Calculating the Pressure Distribution Over Jet-Flapped Wings," R&M No. 3036, 1956, Aeronautical Research Council, London, England.

[2]Maskell, E. C. and Spence, D. A., "A Theory of the Jet Flap in Three Dimensions," *Proceedings of Royal Society of London,* Vol. A251, 1959, pp. 407-425.

[3]Yoler, T. A., "A Lifting Theory of the Jet Flapped Wing," Rept. 24, 1960, Flight Science Laboratory, The Boeing Company.

[4]Lopez, M. L. and Shen, C. C., "Recent Developments in Jet Flap Theory and its Application to STOL Aerodynamic Analysis," AIAA Paper 71-578, Palo Alto, Calif., June 1971.

[5]Das, A., "Tragfluchentheorie fur Traflugel mit Strahklappen," *Jahrbuch der Wissenschaftlichen Gesellschaft fur Luftfahrt,* 1960, pp. 112-133. Translated to: "Lifting Surface Theory for Wings with Jet Flaps," TT 1122, 1964, National Research Council of Canada.

[6]Erickson, J. C. and Kaskel, A. L., "Theoretical Solutions and Numerical Results for Low-Aspect Ratio Rectangular Jet-Flap Control Surfaces," TR 6603, 1966, Therm Advanced Research, Inc.

[7]Tokuda, N., "An Asymptotic Theory of the Jet Flap in Three Dimensions," *Journal of Fluid Mechanics,* Vol. 46, Part 4, 1971, pp. 705-726.

[8]Spence, D. A., "The Lift Coefficient of a Thin Jet-Flapped Wing," *Proceedings of Royal Society of London,* Vol. A238, 1956, pp. 46-68.

[9]Lopez, M. L., Shen, C. C., and Wasson, N. F., "A Theoretical Method for Calculating the Aerodynamic Characteristics of Arbitrary Jet-Flapped Wings, Vol. I—The Elementary Vortex Distribution Jet-Wing Lifting-Surface Theory, Vol. II—EVD Jet-Wing Computer Program User's Manual," Rept. MDC J5519, 1973, Douglas Aircraft Company, Long Beach, Calif.

[10]Shen, C.C., "A Finite-Element Method for Jet-Wing Lifting-Surface Theory," Rept. MDC J5553, Douglas Aircraft Company, Long Beach, Calif.

[11]Das, A., "Theoretische und Experimentelle Untersuchungen an Strahlklappenflugeln, Teil I. Untersuchungen an Rechtechflugeln von Verschiedenen Seitenverhaltnissen," Rept. 61-11, 1961, Institute fur Aerodynamik der DFL; translated to "Theoretical and Experimental Testing on Jet Flap Wings, Part I—Testing of a Rectangular Wing at Various Aspect Ratios," TT F-13,715, 1971, NASA.

[12]Das, A., "Theoretische und Experimentelle Untersuchungen an Tragflugeln endlicher Spannweite mit Strahlklappen," FB 64-40, 1964, Deutsche Forschungsanstalt fur Luft-und Raumfahrt.

[13]Graham, R. R., "Low Speed Characteristics of a 45° Sweepback Wing of Aspect Ratio 8 from Pressure Distributions and Force Tests at Reynolds Numbers from 1,500,000 to 4,800,000," RM L51H13, 1951, NACA.